A Macrobicyclic Calix[6]arene Phosphocine: Conformational Studies Involving High-Resolution NMR Analysis and Molecular Modeling

by **Jean-Bernard Regnouf-de-Vains***[a]), **Alain Cartier**[b]), **Bernard Fenet**[c]), and **Stéphane Pellet-Rostaing**[d])

[a]) GEVSM, UMR 7565 CNRS-UHP, Faculté de Pharmacie, 5, rue Albert Lebrun, BP 403, F-54000 Nancy (phone: +33 383 682315; fax: +33 383 682345; e-mail: jean-bernard.regnouf@pharma.uhp-nancy.fr)

[b]) LCTN, UMR 7565 CNRS-UHP, Faculté des Sciences, F-54000 Vandoeuvre-les-Nancy

[c]) Centre Commun de RMN UCB-CPE, Université Claude Bernard Lyon I, F-69622 Villeurbanne

[d]) LCSO, UMR 5181 CNRS-UCBL, Université Claude Bernard Lyon I, F-69100 Villeurbanne

The solution structure of the phosphorylated hexa(*tert*-butyl)calix[6]arene **1a** was elucidated through a series of high-resolution, one- and two-dimensional ^{1}H- and ^{13}C-NMR experiments, in combination with ^{31}P-NMR measurements. The NMR results were cross-checked and refined with partial structural information obtained from a poorly resolved X-ray crystal-structure analysis. The latter, that could not be upgraded due to the low quality of the crystals and due to strong thermal motions, confirmed that **1a** was a racemate in which two adjacent phenol units are bridged by a mono-ethyl phosphate moiety, generating a macrocyclic dibenzo[1,3,2]-dioxaphosphocine substructure, while the four residual aromatic rings bear regular diethyl phosphate arms. One of these rings is inverted, generating the main asymmetry in the molecule, which gives rise to the racemic nature of the macrobicycle. The two enantiomers, however, do not interconvert on the NMR time scale in solution and resemble the solid-state structure, as expected from the steric hindrance due to the pendant phosphoesters and the high intramolecular tension due to the presence of the phosphocine substructure. The most-probable conformation of **1a** in solution was determined, starting from the NMR and X-ray data, by means of semi-empirical PM3 calculations with the GEOMOS program, including an unprecedented large number of 232 atoms.

Introduction. – Since the pioneering work of *Gutsche* on calixarenes [1], these compounds represent an important class of macrocyclic platforms widely studied for their intrinsic complexation properties as well as for their excellent chemical behavior important for the design of new supramolecular devices. Due to their thermal stability, wide range of complexation of both neutral and ionic guests, and since they can be readily functionalized, calixarenes have become promising chemical platforms for the creation of new synthetic receptors [2].

Main chemical transformations include substitution of the original *t*-Bu groups in *para*-position (upper rim) by H-, Cl-, Br-, and I-atoms, or by SO_3H, NO_2, $ClCH_2$, C=O, or alkyl groups, or, alternatively, at the lower rim, functionalization of the OH groups through esterification or etherification. For example, phosphorylation of the lower-rim OH groups has been developed to access new kinds of selective complexing agents for rare earth species [3] and organic substrates [4]. In parallel, phosphorylations have been developed to access partially-to-fully OH-depleted calixarenes or metacyclophanes [5].

In earlier work [6][7], we reported that hexa(4-*tert*-butyl)calix[6]arene (**1**) can be *O*-phosphorylated such that, on the basis of chemical analyses and preliminary spectroscopic investigations, five phosphoester groups result, four of them being

monodendate, and the fifth bridging either two adjacent (**1a**) or two distant (**1b** or **1c**) lower-rim OH units. Such macrobicyclic structures formally belong to the family of phosphocines, and only a few such rare calixarene analogues have been described in the literature, notably with hexa(4-*tert*-butyl)calix[6]arene [4b] and tetra(4-*tert*-butyl)calix[4]arene [3b], for which a crystal structure is available.

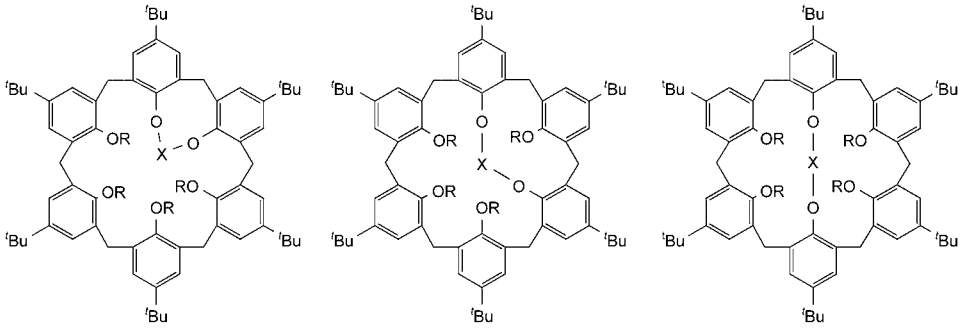

1a **1b** **1c**

X = EtOP(O), R = $(EtO)_2P(O)$

Dibenzo[1,3,2]dioxaphosphocines, analogues of **1a**, showed interesting properties as antibacterials, insecticides, and anticancer agents [8], but also as stabilizers and antioxidants in polymer and oil industries [9]. For these reasons, these rigid, medium-sized heterocyclic compounds have been subjected to intense structural investigations, notably conformational analyses [10].

Due to poor crystal quality and strong thermal motion, our attempts to determine the solid-state structure of compounds **1** gave only inaccurate results that could not be refined to match with the current *Acta Crystallographica* criteria [7]. Nevertheless, our results were sufficient to show that we had isolated compound **1a** (*Fig. 1*), *i.e.*, a macrobicyclic analogue of dibenzo[1,3,2]dioxaphosphocine. We could also show that **1a** consists of two independent symmetrical conformers due to the inversion of one of the four independent phenolic units, which was helpful in the structural and conformational study of the solution structure of this compound by means of high-resolution ^{1}H-, ^{13}C-, and ^{31}P-NMR spectroscopy. The results were, indeed, consistent with those of the X-ray analysis.

We have now re-investigated compound **1a** to determine the most-probable solution structure both by in-depth NMR-spectral analyses and semi-empirical PM3 calculations with the GEOMOS program, which was used for such a large system (232 atoms) for the first time.

Results and Discussion. – 1. *NMR Studies.* 1.1. *Basic Calixarene Framework.* ^{1}H-NMR Spectral analysis of **1a** in CD_2Cl_2 showed that the molecule is rigid enough to display a typical aromatic pattern, with resonances at δ(H) 6.26, 6.29, 6.78, 7.22, 7.40, 7.63, 7.66 and 7.72 (8*d*, $J = 2.2$ Hz each, 1 H each), as well as two broad resonances at δ(H) 7.17 (*s*, 2 H) and 7.25 (*s*, 2 H). The two *doublets* at δ(H) 7.63 and 7.66 seemed to belong to an aromatic *AB* system, representing, thus, one of the six benzene rings. At

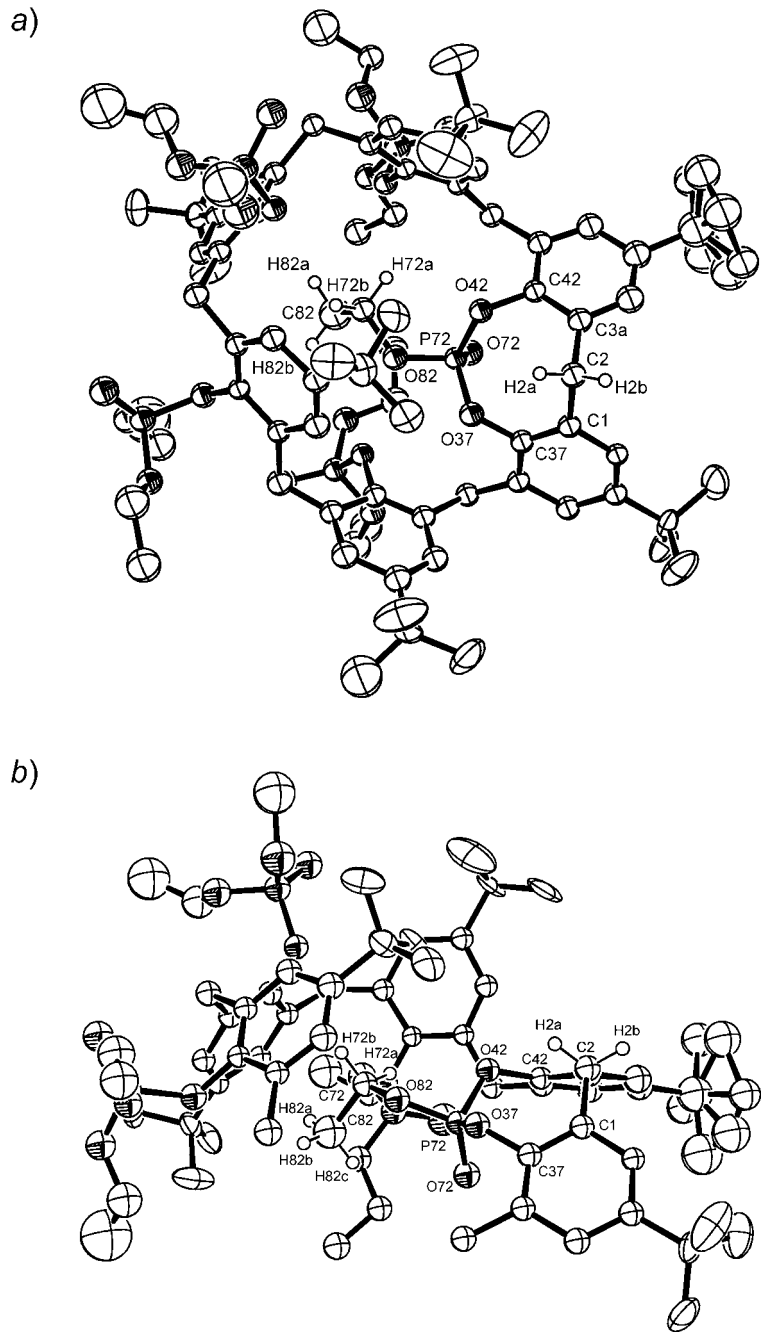

Fig. 1. *Low-resolution X-ray crystal structure of* **1a** (ORTEP numbering and plots at the 50% level). *a*) View of one enantiomer seen from top; *b*) partial side view.

δ(H) 0–2.50, the NMR spectrum of **1a** exhibited six sharp *singlets* due to the *t*-Bu groups, and a complex series of low-intensity signals due to the different Me groups of the pendant ethyl phosphates. Moreover, resonances at δ(H) 0.05 (*t*, 3 H), 0.70 (*m*, 1 H), and 2.36 (*m*, 1 H) were observed. The middle part of the spectrum showed a forest of peaks, probably due to the CH_2 groups of the ethyl phosphates, mixed with a succession of signals shaped as *AB*-type *doublets*, one of them appearing as a 'dedoubled' 1/2 *AB* system ($J_1 = 16.6$, $J_2 = 3.3$ Hz).

Due to the high number of differentiated ^{31}P-coupled C-atoms, the ^{13}C-NMR spectrum of **1a** showed five areas of densely packed signals. The EtO groups appeared at δ(C) 16.00–16.60 (*Me*CH_2O) and 63.00–65.30 (Me*C*H_2O), the *t*-Bu and bridging CH_2 groups appearing at the expected positions, *i.e.*, at δ(C) 30.00–35.50. The ^{13}C-NMR resonances of the bridging CH_2 groups were perfectly separated as six *singlets*. The aromatic region was characterized by a very high density of peaks, which, however, could be all assigned, excepted the *ortho*-C-atoms. The ^{1}H- and ^{13}C-NMR assignments are reported in the *Exper. Part*.

Elucidation of the molecular structure of **1a** in solution required high-resolution NMR techniques. The atomic sequence of the molecule was, thus, elucidated by means of ROESY, HSQC, and HMBC experiments. The ROESY spectrum of **1a** showed that no exchange occured between the two isomers that have to be present in solution. They have, thus, to be considered, on the NMR time scale, as two stable and indistinguishable enantiomers. Couples of aromatic H-atoms and the corresponding *t*-Bu groups have been assigned by this technique, giving rise to six 4-(*tert*-butyl)phenyl units. Their aromatic rings were labeled *A*–*F*, and the aromatic H-atoms, from downfield to upfield, were designated *a*, *c*, *c*′, *b*, *d*, *e*, *d*′, *e*′, *f*, *f*′, *a*′, and *b*′. These rings were then connected with the CH_2 bridges through ROESY experiments, which allowed us to assign four out of six expected *AB* systems; the two residual systems were probably hidden under the forest of peaks due to the ethyl phosphate CH_2 groups. However, ^{1}H,^{13}C-HSQC experiments (*Fig. 2* and *Table 1*) allowed us to unequivocally identify all six *AB* systems, which were labeled $AB_{1,1'}$, $AB_{2,2'}$, $AB_{3,3'}$, $AB_{4,4'}$, $AB_{5,5'}$, and $AB_{6,6'}$ (from upfield to downfield), primed and non-primed indices referring to upfield and downfield 1/2 *AB* systems, respectively. The two hidden *AB* patterns, thus, appear as the compressed $AB_{2,2'}$ and $AB_{6,6'}$ systems (*Table 1*).

Perfectly isolated from the forest of CH_2 peaks, the *AB* systems were finally correlated – with the help of a ^{1}H ,^{13}C-HMBC experiment (*Fig. 3*) – to their adjacent aromatic H-atoms. The intense cross-peaks observed feature the ^3J relationships between the aromatic H-atoms and the quaternary C-atoms of the *t*-Bu groups. All the ^{13}C-NMR resonances, except those of the aromatic C-atoms *ortho* to the OH groups, were thus attributed *via* HMBC. At this stage, the calixarene framework was identified as such (see *Table 1*).

1.2. *Conformational Studies.* Conformational information was obtained through ROESY and ^{31}P-NMR experiments to determine the relative position of each aromatic ring with respect to the central molecular axis. The X-ray crystal structure of **1a** had shown that two adjacent rings were intramolecularly bridged by a phosphate, for which only one residual EtO group had to be expected (in contrast to two such groups for the other phosphate esters). The X-ray data also indicated that one aromatic ring might be conformationally inverted, and that the two bridged ones might be relatively similar in

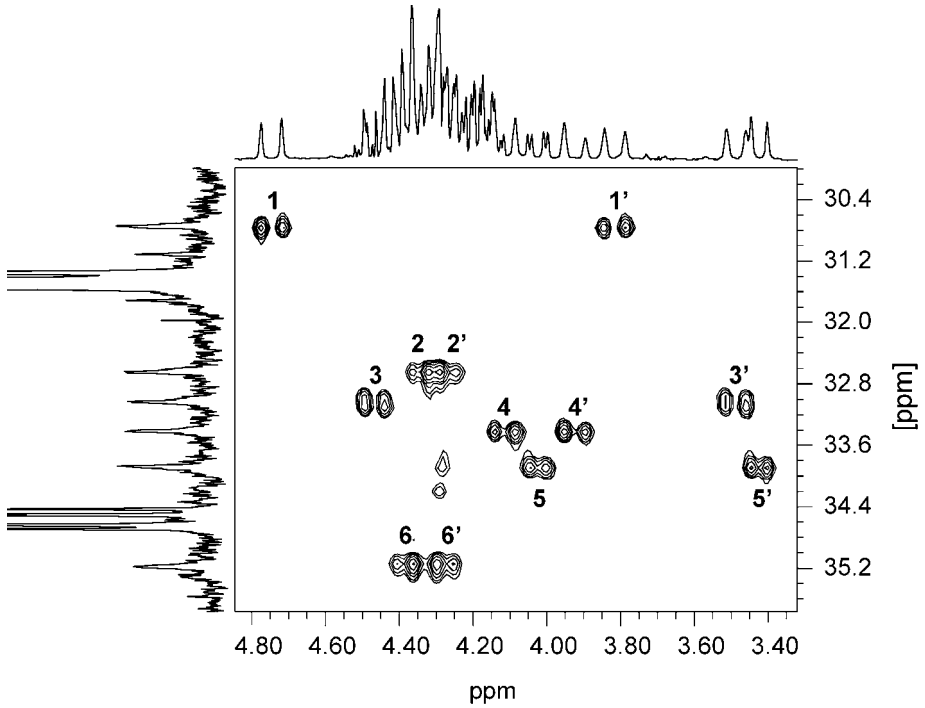

Fig. 2. *Region of the $^{1}H,^{13}C$-HSQC spectrum of* **1a**. Recorded at 300 MHz in CD_2Cl_2 at ambient temperature.

Table 1. *^{1}H-NMR Data* (CD_2Cl_2) *of the Bridging Calixarene CH_2 Resonances in* **1a**

AB	δ(H) [ppm]	*J* [Hz]
1,1′	4.70, 3.77	16.7
2,2′	4.30, 4.22	13.3
3,3′	4.43, 3.44	15.6
4,4′	4.07, 3.88	17.2
5,5′	3.98, 3.37	13.3[a])
6,6′	4.34, 4.23	12.8

[a]) $J(P,H) = 3.3$ Hz.

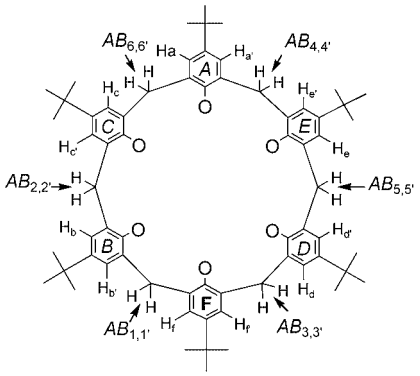

terms of NMR characteristics, and might lie in the average plane of the macrocycle. In addition, ^{1}H-NMR analysis showed that the downfield part of the $AB_{5,5'}$ system was a split *doublet* ($J_{X,H} = 3.3$ Hz), and the aromatic H-atoms of cycles *C*, *D*, and *E* appeared as *AB* systems, while those of rings *A*, *B*, and *F* were of the *AX* type.

The ROESY spectrum of **1a** (*Fig. 4*) showed medium-to-strong interactions between the aromatic H-atoms, and full or half *AB* systems, which were classified according to their intensities (*Table 2*).

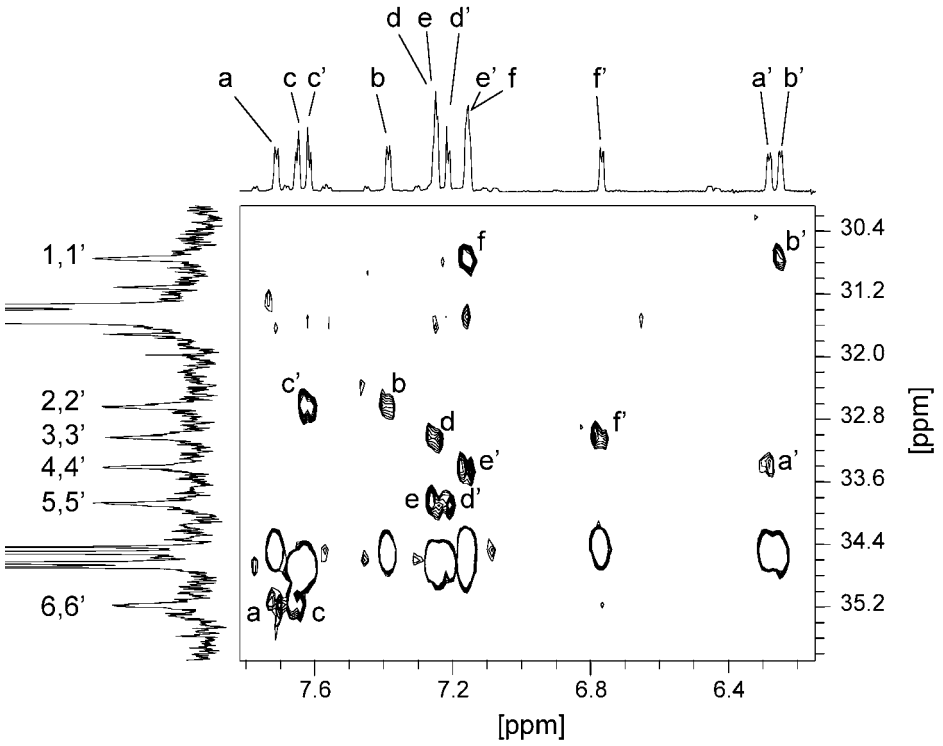

Fig. 3. *Region of the $^{1}H,^{13}C$-HMBC spectrum of* **1a**. Recorded at 300 MHz in CD_2Cl_2 at ambient temperature.

ROE Interactions between adjacent aromatic H-atoms were not found, except between *b′* and *f*, proving a strong distortion of the molecule and confirming that the *B* and *F* rings had the same main orientation. A relatively strong ROE effect was observed between the resonance at δ(H) 0.051 (*t*, 3 H) and both the *AB* system *cc′* (*Fig. 4*) and both the two signals at δ(H) 0.70, 2.36 (2*m*, 1 H each; not visible in *Fig. 4*). In addition, the resonance at δ(H) 0.70 (*m*, 1 H) interacts with the aromatic H-atom *b*. These three signals were assigned to a pendant EtO group, as confirmed by a COSY experiment, looking 'inside' the *C* and *B* aromatic rings, in accordance with their high chemical shifts.

According to the ROESY spectrum of **1a**, only the upfield parts of $AB_{5,5'}$, $AB_{3,3'}$, and $AB_{1,1'}$ interact well with the aromatic H-atoms *d′*, *f′* and *d*, *f*, respectively. $AB_{4,4'}$ interacts symmetrically with *a′* and *e′*, $AB_{2,2'}$ interacts with *c′* and *b*, and $AB_{6,6'}$ interacts with *a* and *c*. These last ambiguous results are due to the presence of a TOCSY effect, which reverberates the answers on both methylene H-atoms inside the *AB* systems. A NOESY experiment performed in this region confirmed that each H-atom of the CH_2 groups is exposed to a different aromatic system. The small spreading of $AB_{2,2'}$ and $AB_{6,6'}$ ($\Delta\delta$ 0.08 and 0.11, resp.) provides significant information on the *quasi*-equivalence of the corresponding H-atoms, thus reinforcing our hypothesis that ring *C* is, indeed, inverted relative to the other five phenols. In addition, the ring *C*

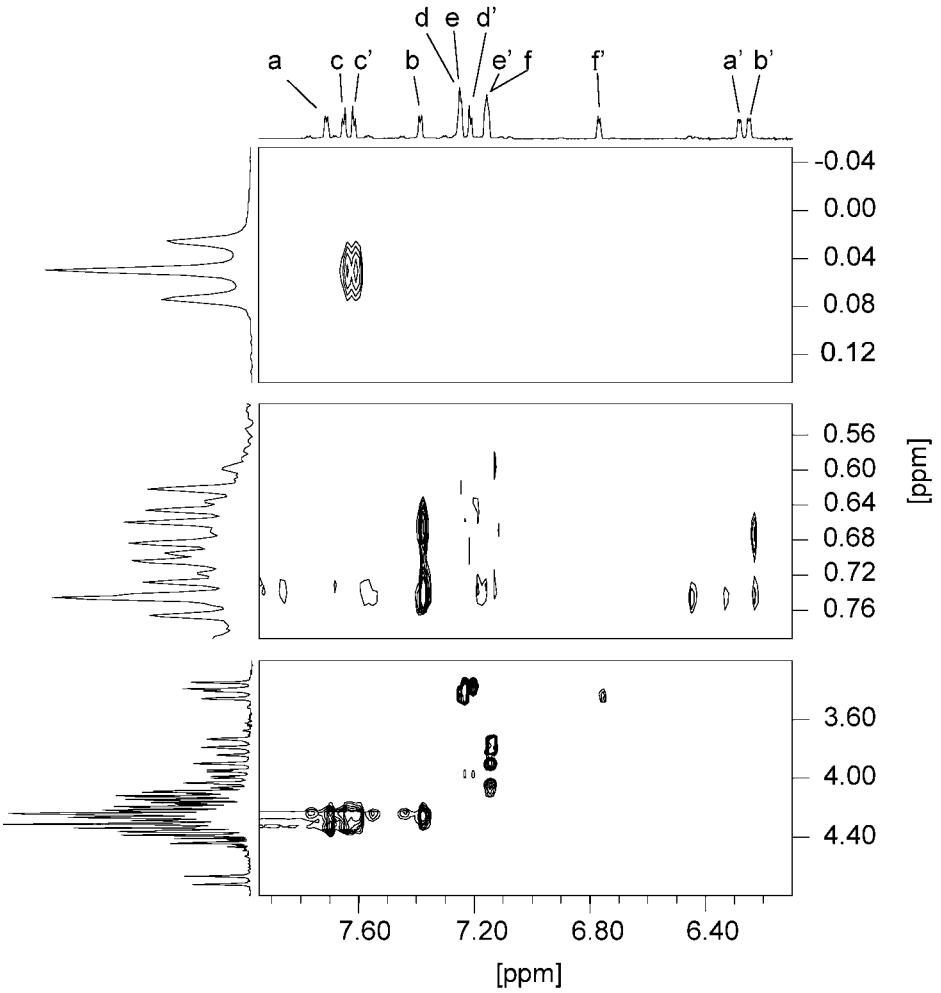

Fig. 4. *ROESY I Interactions between aromatic and aliphatic H-atoms in* **1a**. Recorded at 300 MHz in CD_2Cl_2 at ambient temperature.

Table 2. *Selected ROESY Interactions in* **1a** *between Aromatic H-Atoms and Bridging CH_2 Groups* (*AB* systems). Relative intensities are expressed as 'strong' (*s*) and 'medium' (*m*)

H-Atom	*a*	*b*	*c*	*c′*	*d*	*d′*	*e*	*f*	*f′*
AB System	6,6′	2,2′	6,6′	2,2′	3′	5′	4,4′	1′	3′
Intensity	*s*	*s*	*s*	*s*	*m*	*s*	*s*	*s*	*m*

resonances interacted in a ROESY experiment with the isolated high-field Me group at δ(H) 0.05. For these reasons, we assume that the EtO group pointing towards ring *C* belongs to the *bridging* phosphate. This, thus, should allow us to complete the conformational analysis and signal assignments.

In *Fig. 5*, the ^{1}H-decoupled ^{31}P-NMR spectrum of **1a** is shown. The spectrum clearly exhibits an isolated *singlet* at $\delta(^{31}P)$ −12.32, and four close *singlets* at −4.45, −4.32, −4.25, and −4.00. The latter signals were attributed to the four pendant diethyl phosphate groups, and the former to the bridging phosphoester. *Moran* and *Roundhill* [4b] reported for a similar substructure in a calix[6]arene (but lacking pendant phosphoesters) with a $\delta(^{31}P)$ value of −10.9, and *Byrne et al.*[3b] showed for a similar calix[4]arene that the corresponding bridging *vs.* pendant P-atoms appear at $\delta(^{31}P)$ −6.96 and −3.54, respectively. Finally, the non-decoupled ^{31}P-NMR spectrum of **1a** showed that the *triplet* ($^{3}J_{H,P} = 10$ Hz) was regenerated for each low-field signal, and that the signals at $\delta(^{31}P)$ −12.32 showed a double *doublet* ($^{3}J_{H,P} = 25$ and 6 Hz), which indicated a blocked conformation for the EtOP group.

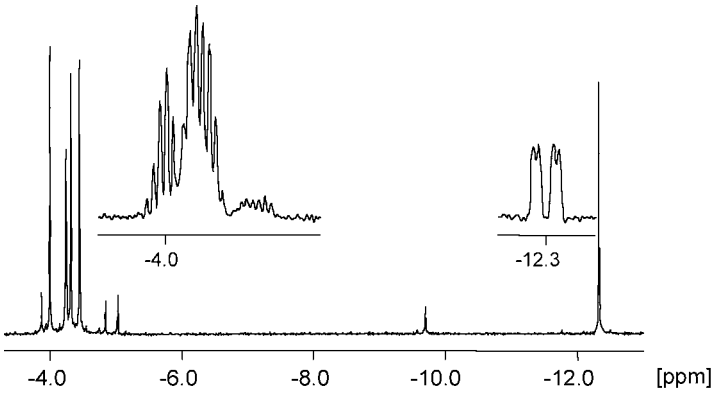

Fig. 5. *^{1}H-Decoupled ^{31}P-NMR spectrum of* **1a**. Insets: non-decoupled signals; recorded at 121.5 MHz in CD_2Cl_2 at ambient temperature.

The ^{1}H-NMR spectrum of **1a**, selectively decoupled from the ^{31}P resonance at −12.32 ppm, showed some modifications in each part of the spectrum. In the high-field region, the two *multiplets* at δ(H) 0.70 and 2.36 became *quartets* ($^{1}J_{H,H} = 10$ Hz), confirming our previous assignment. In the aromatic region, the resonances of the *d*,*d*′ and *e*,*e*′ H-atoms were slightly modified (loss of the small *J* value of 0.4–0.8 Hz). Finally, the $AB_{5,5'}$ system with its *dd*-like down-field part ($J_{AB} = 13.0$, $^{5}J_{X,H} = 3.3$ Hz) became a regular *AB* system ($J_{AB} = 13$ Hz), indicating that the bridging P-atoms were strongly coupled to one H-atom of the linking 5,5′-CH_2 group (*Fig. 6*).

As mentioned in the *Introduction*, the bridging phosphoester substructure formally represents a dibenzo[1,3,2]dioxaphosphocine, and the X-ray crystal structure of **1a** showed that this eight-membered ring has the shape of a *trans*-oriented boat–chair system, as shown in *Fig. 7*. The above-mentioned $^{5}J_{P,H}$ coupling constant has not been reported for cases where the exocyclic substituents of the tetra-coordinated phosphorus are =O and OEt [4b][3b][11], but has been reported for non-calixarene parent structures in which the pendant Et group is replaced by various phenyl groups [9]. According to the literature on phosphocines, this H-atom should be in *endo* position [10c,d], and the observed coupling constants were in agreement with a boat–chair conformation [10b], confirming that the latter is maintained in solution.

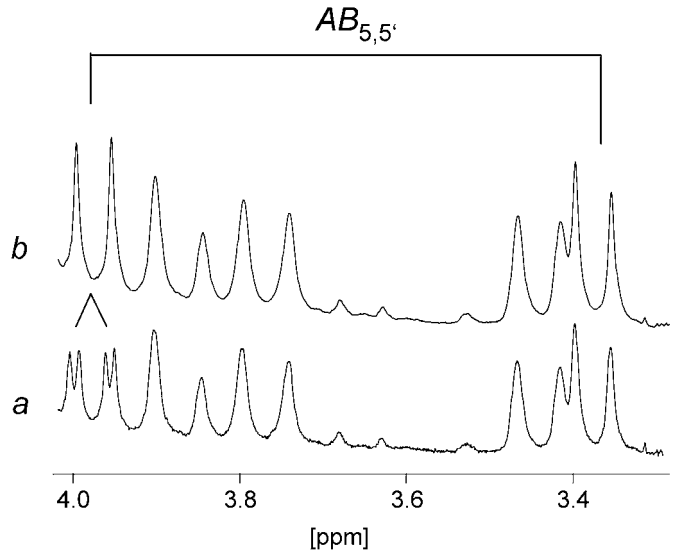

Fig. 6. *Region in the non-decoupled* (lower) *and* ^{31}*P-decoupled* (upper part) ^{1}*H-NMR spectra of* **1a**. Recorded at 300 MHz in CD_2Cl_2 at ambient temperature.

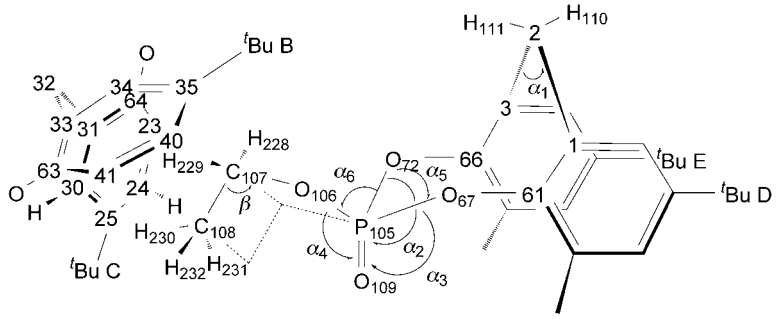

Fig. 7. *Representation of the bridging phosphoester environment in* **1a**. Arbitrary atom numbering according to GEOMOS.

The determination of the inverted and the bridged phenol groups confirmed that the aromatic systems *D* and *E* are bridged by the phosphoester, as shown in the final representation given in *Fig. 8*.

2. *Computational Studies.* The molecular structure of **1a** obtained by X-ray single-crystal analysis was fully optimized by semi-empirical PM3 [12] calculations with an expanded version of the GEOMOS software [13]. Although this program allows computations within a cavity surrounded by a solvent of a given dielectric constant, we had to perform the computations in vacuum due to the large numbers of atoms

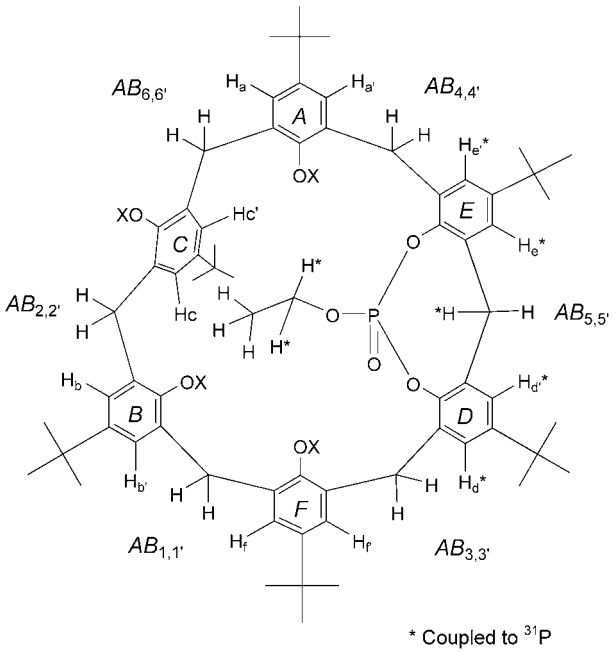

Fig. 8. *Final, structurally and conformationally optimized structure of* **1a**

involved[1]). The minimization led to the reported structure of **1a**, with some conformational changes though, but without strong modifications. The pendant EtO group of the bridging phosphoester was still pointing to the inverted ring *C* (*Fig. 7*), just as in the X-ray (*Fig. 1*) and solution structures (*Fig. 8*). The result that the Me group of the pendant phosphate arm remains in close vicinity to the aromatic *C*-ring H-atoms is in accord with the observed ROE effect (see above). Energy minimization showed that the phosphorus environment ($\alpha_2-\alpha_6$) was highly constrained and distorted in the crystal structure, and that the calixarene bridging CH_2 group forms more or less a right angle, with α_1 (C(2)–H(110)–H(111)) amounting to *ca.* 116° (*Table 3*). Distances between the *C*- and *B*-rings and the Et group are reported in *Table 4*.

Table 3. *Evolution of the Phosphocine Partial Structure of* **1a** *in Terms of Selected Angles.* For definition of angles α, see *Fig. 7* below.

	α_1	α_2	α_3	α_4	α_5	α_6
X-Ray	114.28	114.42	112.77	120.98	106.14	98.50
NMR	115.87	115.67	116.36	114.76	99.86	104.83

It appears that, in the computed structure, H(230) moves away from the *C* ring, while H(228) and H(229) get closer to it. Nevertheless, the pendant Et group always stays in front of the inverted aromatic ring, which rationalizes the observed low NMR

[1]) GEOMOS allows solvent-based energy minimization for organic structures with up to 130 atoms

Table 4. *Variation of the Aromatic 'Environment' of the Phosphocine Type Pendant Ethyl Phosphate H-Atoms in* **1a**. All distances between rings *C* or *B* to the EtO H-atoms in Å; d_{aver} = average distance. For atom numbering, see *Fig. 7*.

To *C*-ring C-atoms							To *B*-ring C-atoms		
X-Ray				NMR			NMR		
Ring	H(228)	H(229)	H(230)	H(228)	H(229)	H(230)	Ring	H(228)	H(229)
C(64)	3.747	3.054	3.226	4.600	4.209	5.864	C(63)	5.821	4.532
C(23)	3.735	3.662	3.045	4.067	3.969	5.096	C(41)	5.930	4.795
C(24)	4.235	4.210	2.746	3.890	3.488	4.168	C(40)	5.844	5.100
C(25)	4.757	4.317	2.729	4.255	3.239	4.112	C(35)	5.608	5.128
C(30)	4.722	3.778	2.910	4.630	3.386	4.920	C(34)	5.367	4.764
C(31)	4.280	3.126	3.179	4.794	3.877	5.739	C(33)	5.468	4.445
d_{aver}	4.246	3.691	2.972	4.373	3.694	4.983		5.673	4.794

chemical shifts of this alkyl group. In fact, discrimination between H(228) and H(229) for NMR assignment is possible based on *Table 4*. Considering that H(229) is essentially looking inside the bent aromatic *B* ring (being closer to ring *C* than H(228)), it was assigned the resonance at δ(H) 0.70 (*m*), in accordance with its previously mentioned ROE interaction with the aromatic *B*-ring H-atoms. Thus, H(228) corresponds to the resonance at δ(H) 2.36 (*m*).

The torsion angles θ_1, θ_2, and β, corresponding to P–O–C–H(228), P–O–C–H(229), and P–O–C–C(108), in the X-ray and solution structure of **1a** are collected in *Table 5*. To rationalize our NMR results, we followed the $^3J_{H,P}$ *vs.* β angle relationship calculated from *Karplus* equations for ^{1}H,^{31}P couplings in phosphoester groups of nucleotides [14]. The following equation is proposed for this case: $^3J(H,P) = 15.3\cos^2\theta - 6.2\cos\theta + 1.5$, which is consistent with a maximum *J* value of 23 Hz (for $\theta = 0$ or 180°). Because our largest coupling constant ($^3J(HCOP) =$ 25 Hz) was higher than theoretically expected, we based our analysis on the lowest one ($^3J_{HCOP} = 6$ Hz). In this case, the following solutions were obtained: $\theta = 67.9$, 141.4, 218.6, and 292.2°.

Table 5. *Variation of Torsion Angles in the Phosphocine Pendant Ethyl Phosphate of* **1a**. θ_1 = P–O–C–H(228); θ_2 = P–O–C–H(229); β = P–O–C–C(108). For atom numbering, see *Fig. 7*.

	θ_1	θ_2	β
X-Ray	330.00°	210.70°	90.4°
NMR	318.42°	203.72°	84.65°

We found that the above two experimental *J* values were consistent with another proposed equation: $^3J_{H,P} = 18.1\cos^2\theta - 4.8\cos\theta$ [15]. For $J = 25$ Hz, θ amounts, thus, to 153.3° and 206.7°, and for $J = 6$ Hz, it becomes 43.7, 316.3, 117.3, and 242.7°. These mathematical solutions were systematically tested for H(229) and H(228), affording logical answers concerning the steric hindrance inside the cavity. Among the 20 available solutions, only five turned out to be consistent with the above 2D-NMR results, as shown with the help of the *Newman* representations **I**–**V** shown in *Fig. 9*.

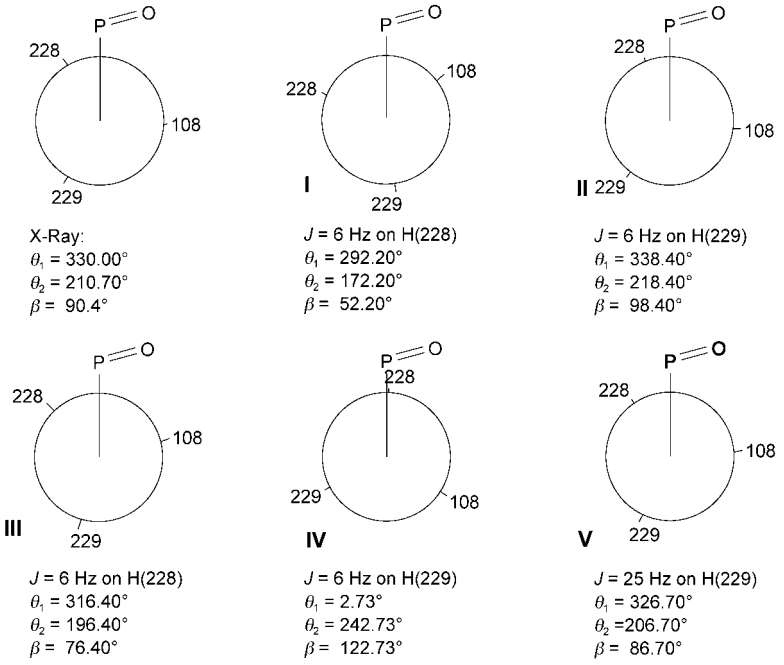

Fig. 9. Newman *Projections of selected Conformers obtained by rotation about the O(106)–C(107) bond in* **1a**. From the different dihedral angles (θ and β), ^3J(H,P) values were calculated *via* the *Karplus* equation based on the following empirical relationships: $^3J = 15.3\cos^2\theta - 6.2\cos\theta + 1.5$ (for **I** and **II**) [14], or $^3J = 18.1\cos^2\theta - 4.8\cos\theta$ (for **III**–**V**) [15]. For definitions of angles, see *Table 5*.

In parallel, we tried to delimit the energetic domains of **1a** by a 30° clockwise rotation of H(228), H(229), and the terminal Me group C(108) about the 0(106)–C(107) bond, thus imposing a constraint of 30° on the β value. The torsion angles of **1a**(1) were found to be close to the values calculated for the structures **II** and **V** (*Fig. 9*). The eleven following conformers **1a**(2)–**1a**(12) thus obtained from **1a**(1) were generated, and their relative energies were compared (*Table 6*).

Comparison of these last results with the *Karplus* solutions showed analogies between conformers **I**/**1a**(12), **II**/**1a**(1–2), **III**/**1a**(12–1), **IV**/**1a**(2–3), and **V**/**1a**(1). Each of the *Karplus* solutions **I**–**V** was then minimized, with a constraint on θ_1 or θ_2, giving the solutions **I′**–**V′**, which were minimized again after removing the initial constraints, finally providing the solutions **I″**–**V″**. The molecular volumes of the conformers **I′**–**V′** and **I″**–**V″** were individually calculated based on the coordinates optimized with GEOMOS and the method described by *Terryn* and *Barriol* [16]. Volumes V, heat of formations E, and dipole moments μ were then calculated for **I″**–**V″** (*Table 7*).

The above five solutions were classified in terms of stability (E), volume (V), and dipole moment (μ). In terms of V, the order **IV″** > **II″** > **V″** > **I″** > **III″** was derived; regarding μ, the sequence **V″** > **IV″** > **II″** > **III″** > **I″** was obtained; and with respect to E, the order **V″** (−1152.132) > **II″** (−1152.019) > **III″** (−1151.958) > **IV″**

Table 6. *Change in Relative Energy* (ΔE) *upon Variation of Torsion Angles in* **1a** *by a Clockwise 30°-Rotation Constraint on* β. For torsion-angle definitions and atom numberings, see *Table 5* and *Fig 7*, resp.

Conformer	β [°]	θ_1 [°]	θ_2 [°]	ΔE [kcal/mol]
1a(1)	84.65	318.42	203.72	0
1a(2)	114.65	349.85	233.79	+1.147
1a(3)	144.65	22.63	264.65	+0.303
1a(4)	174.65	53.79	295.31	+2.372
1a(5)	204.65	84.92	327.26	+1.483
1a(6)	234.65	114.14	358.06	+1.726
1a(7)	264.65	143.75	29.59	+1.770
1a(8)	294.65	174.66	60.70	+0.427
1a(9)	324.65	202.04	89.38	+2.048
1a(10)	354.65	230.79	117.96	+4.361
1a(11)	24.65	259.75	147.23	+6.813
1a(12)	54.65	288.83	174.92	+2.040

Table 7. *Calculated Molecular Volume* (V [Å^3]), *Heat of Formation* (E [kcal/mol]), *and Dipole Moment* (μ [D]) *of the* Karplus *Derived Conformers* **I**–**V** *of* **1a**, *and of the Second- and Third-Generation Minimized Conformers* **I′ – V′** *and* **I″ – V″**, *resp.* For definitions of angles, see *Table 5*.

	I	**II**	**III**	**IV**	**V**
θ_1	292.20[a])	338.40	316.40[a])	2.73	326.70
θ_2	172.20	218.40[a])	196.40	242.73[a])	206.70[a])
β	52.20	98.40	76.40	122.73	86.70
V	1650.927	1660.663	1709.849	1660.721	1671.82
	I′	**II′**	**III′**	**IV′**	**V′**
θ_1	292.20[b])	334.177	316.40[b])	−1.858	322.514
θ_2	178.292	218.40[b])	200.881	242.73[b])	206.70[b])
β	58.429	99.060	82.383	122.666	87.972
V	1650.286	1667.502	1644.022	1669.586	1654.893
E	−1150.427	−1152.019	−1151.956	−1150.982	−1152.119
	I″	**II″**	**III″**	**IV″**	**V″**
θ_1	292.286	334.177	316.279	−1.900	322.605
θ_2	178.300	218.395	200.867	242.360	207.234
β	58.433	99.061	82.373	122.603	88.090
V	1650.293	1667.495	1643.952	1670.447	1657.422
E	−1150.428	−1152.019	−1151.958	−1151.017	−1152.132
μ	3.54841	3.89850	3.75272	4.02566	4.14221

[a]) Exper. values. [b]) Fixed values

(−1151.017) > **I″** (−1150.428) was obtained, corresponding to ΔE values of 0.113, 0.061, 0.935, and 0.589 kcal/mol, respectively.

The above NMR studies with **1a** were performed in solution (CD_2Cl_2). According to the *Onsager* reaction-field model [17], the conformer for which the ratio μ^2/V has the highest value is the most-favored one, as long as higher-order moments, compared to μ, are not too large. Thus, the conformer **V″** ($\mu^2/V = 0.01035$ D^{2}Å^{-3}), which was found to be the most stable rotamer in vacuum, was assumed to be the most stable one in solution as well.

For the five final conformers **I″**–**V″**, the average distances between H(230), H(229), H(228), and the aromatic rings *B* and *C* were calculated (*Table 8*). In conclusion, **V″** appears to be the best candidate for the solution structure of **1a**.

Table 8. *Distances between Selected H-Atoms and Ring*-B *and* -C *Atoms in Conformers* **I″**–**V″**. Average distances are referred to as d_{aver}.

	Ring *C*	H(228)	H(229)	H(230)	Ring *B*	H(228)	H(229)
V″	C(64)	5.272	4.545	6.599	C(63)	6.478	5.253
	C(23)	4.650	4.090	5.748	C(41)	6.499	5.473
	C(24)	4.402	3.512	4.888	C(40)	6.372	5.709
	C(25)	4.784	3.413	4.973	C(35)	6.170	5.695
	C(30)	5.258	3.815	5.825	C(34)	6.013	5.354
	C(31)	5.496	4.369	6.588	C(33)	6.163	5.117
	d_{aver}	4.977	3.957	5.770	d_{aver}	6.283	5.434
II″	C(64)	5.148	4.183	6.008	C(63)	6.345	4.927
	C(23)	4.570	3.832	5.210	C(41)	6.391	5.199
	C(24)	4.351	3.372	4.283	C(40)	6.257	5.399
	C(25)	4.705	3.266	4.247	C(35)	6.023	5.307
	C(30)	5.129	3.530	5.083	C(34)	5.843	4.916
	C(31)	5.349	3.991	5.912	C(33)	6.002	4.708
	d_{aver}	4.875	3.696	5.124	d_{aver}	5.673	4.794
III″	C(64)	4.622	4.444	6.030	C(63)	5.821	4.532
	C(23)	4.094	4.170	5.211	C(41)	5.930	4.795
	C(24)	3.856	3.586	4.289	C(40)	5.844	5.100
	C(25)	4.145	3.235	4.281	C(35)	5.608	5.128
	C(30)	4.537	3.451	5.143	C(34)	5.367	4.764
	C(31)	4.773	4.070	5.962	C(33)	5.468	4.445
	d_{aver}	4.338	3.826	5.153	d_{aver}	5.673	4.794
IV″	C(64)	5.522	3.943	5.665	C(63)	6.496	4.952
	C(23)	4.943	3.587	4.923	C(41)	6.472	5.195
	C(24)	4.732	3.396	4.026	C(40)	6.374	5.273
	C(25)	5.103	3.572	3.970	C(35)	6.245	5.078
	C(30)	5.506	3.768	4.728	C(34)	6.135	4.701
	C(31)	5.712	3.955	5.529	C(33)	6.258	4.626
	d_{aver}	5.253	3.704	4.807	d_{aver}	6.330	4.971
I″	C(64)	6.142	4.956	6.067	C(63)	6.094	4.671
	C(23)	3.765	4.509	4.897	C(41)	5.352	5.091
	C(24)	3.618	3.862	4.132	C(40)	5.311	5.476
	C(25)	3.815	3.466	4.369	C(35)	5.064	5.624
	C(30)	4.037	3.709	5.232	C(34)	4.762	5.321
	C(31)	4.200	4.395	5.890	C(33)	4.818	4.942
	d_{aver}	4.263	4.149	5.098	d_{aver}	5.233	5.187

3. Conclusions. – To overcome the impossibility to resolve correctly the raw X-ray crystal structure of the calix[6]arene pentaphosphate **1a**, its structure has been re-analyzed spectroscopically in solution as well as by computer modeling. The molecular frame was rebuilt, and the most-probable conformation was recovered through high-resolution, one-dimensional ^{1}H-, ^{13}C-, and ^{31}P-NMR, and *via* two-dimensional NOESY, ROESY, HSQC, and HMBC techniques. Four regular pendant ethyl phosphates plus

one intramolecularly bridging phosphate, making up an eight-membered cyclophosphoester substructure, were identified. The presence of the bridging phosphoester group, spanning two adjacent phenol units, resulted in specific ^{1}H- and ^{31}P-resonances and couplings, notably a long-range ^5J(P,H) coupling between the calixarene bridging CH_2 H-atoms and the corresponding P-atom, and two ^3J(H,P) couplings between the P-atom and the CH_2 unit of the residual pendant Et group; the latter were useful in the determination of a more-precise structure of **1a** in solution. Thus, the resolution of the ^3J(H,P) *Karplus* equation afforded various phosphocine analogous conformations, which were more precisely analyzed with the GEOMOS program, giving rise to the five finally optimized conformers **I″**–**V″** of equivalent energies, and displaying limited conformational changes with regards to the molecule in the crystal. Each of these conformers was finally classified with respect to energy, volume and dipole moment, leading to **V″** as the best candidate to feature the CD_2Cl_2 solution structure of **1a**.

We are grateful to MRES and CNRS for financial support, to *M. Perrin*, *S. Lecocq*, and *C. Bavoux* for X-ray measurements, and to *Nicole Marshall* for correcting the manuscript.

Experimental Part

General. ^{1}H-, ^{13}C-, and ^{31}P- NMR Spectra: *Bruker AM 300* (300, 75.46, and 121.49 MHz, resp.); chemical shifts δ in ppm, coupling constants J in Hz. All experiments, except COSYLR and HMBC, were performed in the phase-sensitive mode. For COSYDQF, HSQC, and HMBC, gradients were used for coherence selection. The acquisition parameters for ROESY were: $SW = 2994$ Hz, $SI = 2$ k; $D_1 = 1.5$ s, mixing time $t_m = 250$ ms, with $(\gamma/2\pi)\,B_1 = 2$ kHz; $NE = 512$ increments (second dimension). Data were processed with the Felix 2.0 package in the phase-sensitive mode, using a square sine-bell window function in the two dimensions, and a final matrix size of 1k × 1k of reals. Parameters for gradient HMBC: SW (^{1}H) = 2994 Hz, $SI = 1$ k, $D_1 = 1.5$ s, SW (^{13}C) = 12077 Hz, NE = 512; Z gradient = 6 G cm^{-1}. Data were processed with the Felix 2.0 package in the absolute mode, with a 90° shifted square sine bell in the two dimensions, and a final matrix size of 1k × 1k of reals.

Data of **1a**. M.p. 218–219°. IR (KBr): 964, 1030, 1180, 1273 (phosphoester). UV ($CHCl_3$) : 276.2 (2770); 271.0 (2508). ^{1}H-NMR (CD_2Cl_2): 0.051 (*t*, $J = 9.5$, *Me*CH$_2$O); 0.64–0.76 (*m*, 1 H of MeC*H*$_2$O); 0.916 (*s*, *t*-Bu (*B*)); 1.133 (*s*, *t*-Bu (*A*)); 1.185 (s, *t*-Bu (*F*)); 1.288 (*s*, *t*-Bu (*E*)); 1.318 (*s*, *t*-Bu (*D*)); 1.38 (s, *t*-Bu (*C*)); 2.26–2.42 (*m*, 1 H of MeC*H*$_2$O); 3.37 (*d*, 1/2 *AB*, $J_{AB} = 13.3$, 1 H of ArC*H*$_2$Ar (5,5′)); 3.98 (*d*, 1/2 *AB*, $J_{AB} = 16.6$, ^5J(P,H) = 3.3, 1 H of ArC*H*$_2$Ar (5,5′)); 3.44, 4.43 (*AB*, $J_{AB} = 15.6$, ArC*H*$_2$Ar (3,3′)); 3.77, 4.70 (*AB*, $J_{AB} = 16.7$, ArC*H*$_2$Ar (1,1′)); 3.88, 4.07 (*AB*, $J_{AB} = 17.2$, ArC*H*$_2$Ar (4,4′)); 4.22, 4.30 (*AB*, $J_{AB} = 13.3$, ArC*H*$_2$Ar (2,2′)); 4.23, 4.34 (*AB*, $J_{AB} = 12.8$, ArC*H*$_2$Ar (6,6′)); 6.26 (*d*, $J = 2.2$, H$_{b'}$); 6.29 (*d*, $J = 2.2$, H$_{a'}$); 6.78 (*d*, $J = 2$, H$_{f'}$); 7.16 (*d*, $J = 2$, H$_f$); 7.17 (*d*, $J = 2.2$, H$_{e'}$); 7.22 (*d*, $J = 2.1$, H$_{d'}$); 7.25 (*d*, $J = 2.2$, H$_e$); 7.26 (*d*, $J = 2.1$, H$_d$); 7.40 (*d*, $J = 2.2$, H$_b$); 7.63 (*d*, $J = 2$, H$_{e'}$); 7.66 (*d*, $J = 2$, H$_c$); 7.72 (*d*, $J = 2.2$, H$_a$). ^{13}C-NMR (CD_2Cl_2): 16.16 (bridged *Me*CH$_2$OP); 16.20–16.55 (*m*, (*Me*CH$_2$O)$_2$P); 31.36 (*Me*$_3$C (*A*)); 31.29 (*Me*$_3$C (*B*)); 31.45 (*Me*$_3$C (*C*)); 31.475 (*Me*$_3$C (*D,E*)); 31.398 (*Me*$_3$C (*F*)); 30.68 (Ar*C*H$_2$Ar (1,1′)); 32.57 (ArCH$_2$Ar (2,2′)); 32.97 (Ar*C*H$_2$Ar (3,3′)); 33.35 (Ar*C*H$_2$Ar (4,4′)); 33.80 (Ar*C*H$_2$Ar (5,5′)); 35.11 (Ar*C*H$_2$Ar (6,6′)); 34.36 (Me$_3$*C* (*F*)); 34.425 (Me$_3$*C* (*A*)); 34.44 (Me$_3$*C* (*B*)); 34.57 (Me$_3$*C* (*D,E*)); 34.62 (Me$_3$*C* (*C*)); 63.44 (*d*, J(P,C) = 5, bridged Me*C*H$_2$OP); 64.50–65.30 (8*d*, J(P,C) = 5.6, (Me*C*H$_2$O)$_2$P); 124.20 (*d*, J(P,C) = 1.7, H$_{a'}$–C); 125.22 (*d*, J(P,C) = 1.9, H$_{f'}$–C); 125.50 (*d*, J(P,C) = 1.6, H$_{d'}$–C); 125.95 (*d*, J(P,C) = 1.7, H$_e$–C); 126.24 (*d*, J(P,C) = 2.0,H$_{b'}$–C); 126.87 (*d*, J(P,C) = 1.7, H$_b$–C); 125.46 (*d*, J(P,C) = 1.9, H$_d$–*C*); 128.48 (*d*, J(P,C) = 1.7, H$_a$–C, H$_{e'}$–C); 128.67 (*d*, J(P,C) = 2.1, H$_f$–C); 129.06 (*d*, J(P,C) = 1.7, H$_{e'}$–C); 129.40 (*d*, J(P,C) = 1.8, H$_c$–C); 129.70 (*d*, J(P,C) = 3.3); 130.70 (*d*, J(P,C) = 4.6); 131.13 (*d*, J(P,C) = 0.9); 131.55 (*dd*, J(P,C) = 1.3, 3.3); 131.84 (*d*, J(P,C) = 3.2); 132.09 (*dd*, J(P,C) = 1.0, 3.2); 132.25 (*dd*, J(P,C) = 0.9, 3.5); 132.82 (*d*, J(P,C) = 3.5); 132.96 (*d*, J(P,C) = 3.8); 133.35 (*dd*, J(P,C) = 1.0, 3.5); 133.87 (*d*, J(P,C) = 3.1); 134.18 (*d*, J(P,C) = 4.6); (*o*-C of Ar); 147.18 (*d*, J(P,C) = 2.3, *p*-C of *F*); 147.40 (*d*, J(P,C) = 2.3, *p*-C of *B*); 147.54 (*d*, J(P,C) = 2.2, *p*-C of *A*); 147.81 (*d*, J(P,C) = 2.3, *p*-C of *C*); 148.65 (*d*, J(P,C) = 2.2, *p*-C of *D*); 148.91 (*d*, J(P,C) = 2.0, *p*-C of *E*); 144.48 (*d*, J(P,C) = 5.7, C$_i$ of *D*); 144.92 (*d*, J(P,C) = 7.9, C$_i$ of *B* and *F*); 144.98 (*d*, J(P,C) = 7.7, C$_i$ of *E*); 146.295 (*d*, J(P,C) = 7.5, C$_i$ of *C*); 146.97 (*d*, J(P,C) = 7.6, C$_i$ of *A*). MS: 1629.6 ([*M* + Na]$^+$). Anal. calc. for $C_{84}H_{123}O_{20}P_5$ (1607.66): C 62.75, H 7.77, O 19.90; found: C 62.67, H 7.74, O 19.69. X-Ray Crystallography: see *Fig. 1*. Crystallographic data (excluding structure factors) for **1a** have been deposited with

the *Cambridge Crystallographic Data Centre* as supplementary publication number CCDC-220240. Copies of the data can be obtained, free of charge, on application to *CCDC*, 12 Union Road, Cambridge CB2 1EZ, UK (+44-1223-336-033; e-mail: data_request@ccdc.cam.ac.uk), or *via* the internet (http://www.ccdc.cam.ac.uk/data_request/cif).

REFERENCES

[1] C. D. Gutsche, 'Calixarenes', Monographs in Supramolecular Chemistry, Ed. J. F. Stoddart, Royal Society of Chemistry, Cambridge, 1989.

[2] 'Calixarenes: A Versatile Class of Macrocyclic Compounds', Eds. J. Vicens, V. Böhmer, Kluwer, Dordrecht, 1991; C. D. Gutsche, 'Calixarenes Revisited', Royal Society of Chemistry, Cambridge, 1998; 'Calixarenes 2001', Eds. Z. Asfari, V. Böhmer, J. Harrowfield, J. Vicens, Kluwer, Dordrecht, 2001.

[3] a) D. M. Roundhill, E. Georgiev, A. Yordanov, *J. Inclusion Phenom. Mol. Recognit. Chem.* **1994**, *19*, 101; b) L. T. Byrne, J. M. Harrowfield, D. C. R. Hockless, B. J. Peachey, B. W. Skelton, A. H. White, *Aust. J. Chem.* **1993**, *46*, 1673.

[4] a) L. N. Markovskii, V. I. Kal'chenko, N. A. Parkhomenko, *Zh. Obshch. Khim.* **1990**, *60*, 2811; b) J. K. Moran, D. M. Roundhill, *Phosphorus Sulfur Silicon Relat. Elem.* **1992**, *71*, 7; c) R. G. Jansen, W. Verboom, S. Harkema, G. J. van Hummel, D. N. Reinhoudt, A. Pochini, R. Ungaro, P. Prados, J. de Mendoza, *J. Chem. Soc., Chem Commun.* **1993**, 506; d) F. Grynszpan, O. Aleksiuk, S. E. Biali, *J. Chem. Soc., Chem Commun.* **1993**, 13; e) T.-N. Ursales, I. Silaghi-Dumitrescu, *Rev. Roum. Chim.* **2004**, *49*, 437.

[5] Z. Goren, S. E. Biali, *J. Chem. Soc., Perkin Trans 1* **1990**, 1484; Y. Ting, W. Verboom, L. C. Groenen, J. -D. van Loon, D. N. Reinhoudt, *J. Chem. Soc., Chem. Commun.* **1990**, 1432; F. Grynszpan, Z. Goren, S. E. Biali, *J. Org. Chem.* **1991**, *56*, 532.

[6] J.-B. Regnouf-de-Vains, S. Pellet-Rostaing, R. Lamartine, *Tetrahedron Lett*. **1994**, *35*, 8147.

[7] J.-B. Regnouf-de-Vains, R. Lamartine, S. Pellet-Rostaing, M. Perrin, A. Thozet, S. Lecocq, in 'Supramolecular Stereochemistry', NATO ASI Series, Ed. J. S. Siegel, Kluwer, Dordrecht, 1995, Series C, Vol. 473, p 227.

[8] K. Ananda Kumar, C. Suresh Reddy, N. Jagadeesh Kumar, M. Krishnaiah, *Phosphorus Sulfur Silicon Relat. Elem.* **2001**, *173*, 83, and refs. cit. therein.

[9] M. Venugopal, C. Devendranath Reddy, *Heteroat. Chem.* **2001**, *12*, 10.

[10] a) O. I. Danilova, R. P. Arshinova, O. V. Ovodova, B. A. Arbuzov, *Zh. Obshch. Khim.* **1987**, *57*, 2679; b) R. P. Arshinova, O. I. Danilova, B. A. Arbuzov, *Phosphorus Sulfur Silicon Relat. Elem.* **1987**, *34*, 1; c) J. D. Goddard, A. W. Payne, N. Cook, H. R. Luss. *J. Heterocycl. Chem*. **1988**, *25*, 575; d) H. S. Rzepa, R. N. Sheppard, *J. Chem. Research, Synop.* **1988**, 102; d) S. Kumaraswamy, K. Senthil Kumar, S. Raja, K. C. Kumara Swamy, *Tetrahedron* **2001**, *57*, 8181.

[11] 'Handbook of Phosphorus-31 Nuclear Magnetic Resonance Data', Ed. J. C. Tebby, CRC Press, Boca Raton, 1991.

[12] J. J. P. Stewart, *J. Comput. Chem.* **1989**, *10*, 209.

[13] D. Rinaldi, P. E. Hoggan, A. Cartier, GEOMOS (Q.C.P.E. 584), *QCPE Bull.* **1989**, *9*, 128.

[14] S. S. Wijmenga, M. M. W. Mooren, C. W. Hilbers, in 'Multidimensional NMR in Structural Biology', EMBO Practical Course, Torino, Italy, 1995, p 217.

[15] L. D. Quin, in 'Methods in Stereochemical Analysis 8. ^{31}P-NMR Spectroscopy in Stereochemical Analysis. Organic Compounds and Metal Complexes', Eds. J. G. Verkade, L. D. Quin, VCH Publishers, Deerfield Beach, 1987, p 366.

[16] B. Terryn, J. Barriol, *J. Chim. Phys.* **1981**, *78*, 207.

[17] L. Onsager, *J. Am. Chem. Soc.* **1936**, *58*, 1486.

Received February 24, 2005